

# A Digital Control of Power Leveling Unit with Super Capacitor for Distributed Generator

Shin-ichi Hamasaki\*, Sho Yoshioka \*, and Mineo Tsuji \*

\* Nagasaki University, 1-14 Bunkyo-machi, Nagasaki, 852-8521, Japan

**Abstract** — The power leveling (PL) unit is required to maintain a balance of power flow for photovoltaic (PV) system. It is important for it to respond quickly against fluctuation of power generation. A new control scheme based on discrete time system for the PL unit in the distributed generator (DG) is proposed to improve the response. In the proposed method, the deadbeat control is performed using state equations obtained from a combination of two-quadrant chopper and super capacitors. The optimal duty ratio of PWM can be calculated and good performance of the current regulation is obtained. The control theory and the simulation results are presented in this paper.

**Index Terms** — distributed generator, super capacitor, power leveling, deadbeat control

## I. INTRODUCTION

In recent years, distributed power of solar and wind power generation has become widespread. DC power supply system as represented by DC micro-grid attracts attention. However an output fluctuation often occurs and may cause occurrence of reverse power flow, voltage regulation problem, an increase of harmonic current, and impacts on system frequency. The DC micro grid consists of the distributed generator (DG), loads, and energy storage elements in the DC distribution. Therefore, several types of power leveling (PL) unit with a battery or a capacitor in the distributed generator have been proposed and developed[1]-[5].

In this paper, a digital deadbeat based control[6] for PL unit is proposed for stable power supply considering the grid-connection of DG with a PV system. The PL unit consists of a two-quadrant DC chopper and a super capacitor as high capacity storage. The DG system has a grid-connected inverter which can determine active and reactive current to the AC line voluntarily and the active and reactive components are controlled independently. On the DC bus, boost type chopper is provided on the output side of the PV system, by which an output power can be controlled taking into account the characteristics of PV cells. The inverter and the PL unit can be controlled cooperatively to regulate active power flow and the DC-bus voltage according to the PV output power. DC bus voltage of the inverter is maintained constant, because the PL unit can operate the leveling quickly for instantaneous fluctuation of power generation by using the digital dead beat control of the chopper.

To verify whether the PL unit can properly perform

power leveling in case of charge or discharge of the super capacitor and to clarify the effectiveness of the proposed method, simulations in several situations are performed.

## II. CONTROL METHOD

### A. Main Circuit Configuration

Fig.1 shows a circuit for analysis. The DG is connected parallel to the power line ( $v_s$ ,  $L_s$ ,  $R_s$ ). The PL unit is configured with a super capacitor, a reactor and a two-quadrant chopper. A grid-connected inverter is to control the rate of power supply to the load side of the AC line. The power control is performed to stabilize the DC system voltage and power variation absorption of the PV system. This study is conducted as the following steps.

1. Input or output power control of PL unit / Constant control of the DC bus voltage
2. Control of active and reactive power of the AC bus by the inverter

### B. Active and reactive power control

The detected three-phase current and voltage are transformed to the d-q axis value by the d-q transform described in (1).

$$\begin{bmatrix} i_d \\ i_q \end{bmatrix} = \sqrt{\frac{2}{3}} \begin{bmatrix} \sin \theta & \sin \left( \theta - \frac{2}{3} \pi \right) & \sin \left( \theta + \frac{2}{3} \pi \right) \\ \cos \theta & \sin \left( \theta - \frac{2}{3} \pi \right) & \cos \left( \theta + \frac{2}{3} \pi \right) \end{bmatrix} \begin{bmatrix} i_u \\ i_v \\ i_w \end{bmatrix} \quad (1)$$

Fig.2 shows the definitions of the d-q axis and  $\theta$ .  $\theta_u$  is a phase of u-phase voltage  $v_u$  and calculated from the phase  $\theta_{uv}$  of line-to-line voltage by (2).

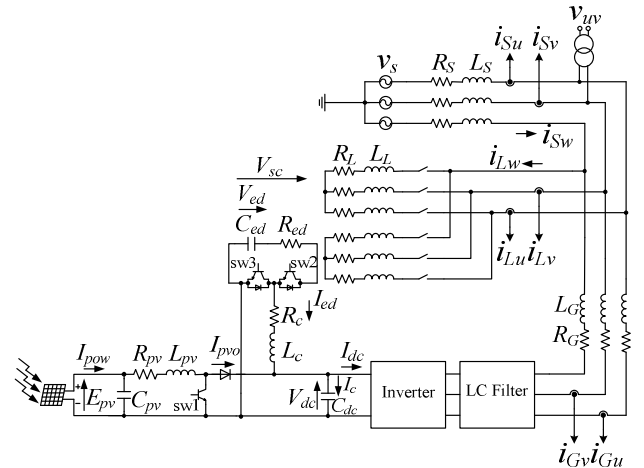


Fig.1 Circuit configuration

$$\theta_u = \theta_{uv} - \frac{\pi}{6} \quad (2)$$

Here the line voltages are defined as (3)-(5).

$$v_u = \sqrt{\frac{2}{3}}V \sin \theta_u \quad (3)$$

$$v_v = \sqrt{\frac{2}{3}}V \sin \left( \theta_u - \frac{2}{3}\pi \right) \quad (4)$$

$$v_w = \sqrt{\frac{2}{3}}V \sin \left( \theta_u + \frac{2}{3}\pi \right) \quad (5)$$

Then voltages  $v_d$  and  $v_q$  are calculated by (1).

$$v_d = V \quad (6)$$

$$v_q = 0 \quad (7)$$

The active power  $P$  and the reactive power  $Q$  are obtained in Fig.2.

$$P = v_d i_d + v_q i_q \quad (8)$$

$$Q = v_d i_q - v_q i_d \quad (9)$$

(10) and (11) are derived from (6)-(9).

$$P = VI_d \quad (10)$$

$$Q = VI_q \quad (11)$$

(10) and (11) means that the active power  $P$  and the reactive power  $Q$  is depend on  $i_d$  and  $i_q$  respectively. Thus  $i_d$  is called an active current and  $i_q$  is called an reactive current.

Fig.3 illustrates a block diagram of the active and the reactive power control of the DG. The control law becomes (12) and (13).

$$V_{Gd}^* = V_{Gd} + K_{pd} (I_{Gd}^* - I_{Gd}) + K_{id} \int_0^t (I_{Gd}^* - I_{Gd}) dt \quad (12)$$

$$V_{Gq}^* = V_{Gq} + K_{pq} (I_{Gq}^* - I_{Gq}) + K_{iq} \int_0^t (I_{Gq}^* - I_{Gq}) dt \quad (13)$$

Active and reactive powers on the AC line are controlled to consume all the generated power obtained from the PV system or to minimize the power consumption of the main power line[4].

### C. Control Method in DC Side

Fig.4 shows the relationship of the power flow in the DC side. All the power flow must be balanced properly by the control of the PL unit.

The active power  $P$  of the DG satisfies (14).

$$P = VI_{Gd} = V_{dc} I_{dc} \quad (14)$$

Further power flow balance satisfies (15) in Fig.4.

$$V_{dc} I_{ed} + V_{dc} I_{pvo} - V_{dc} I_c = V_{dc} I_{dc} \quad (15)$$

All the currents on the DC bus should be balanced as shown in (16).

$$I_{ed} = I_{dc} + I_c - I_{pvo} \quad (16)$$

The DC current reference  $I_{dc}^*$  of the inverter can be obtained by (14).

$$I_{dc}^* = \frac{VI_{Gd}}{V_{dc}} \quad (17)$$

When the super capacitor supplies the power, the DC/DC two-quadrant chopper works as a buck converter by the PWM control. When the super capacitor is charged the power, the DC chopper works as a boost converter by the PWM control.

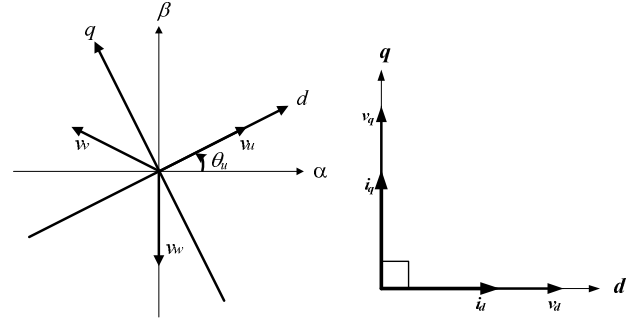


Fig.2 Definition of d-q axis

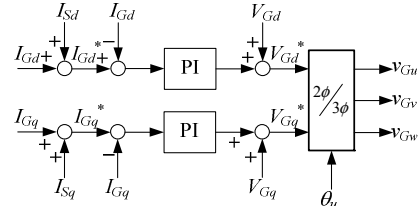


Fig.3 Block diagram of the control of inverter side

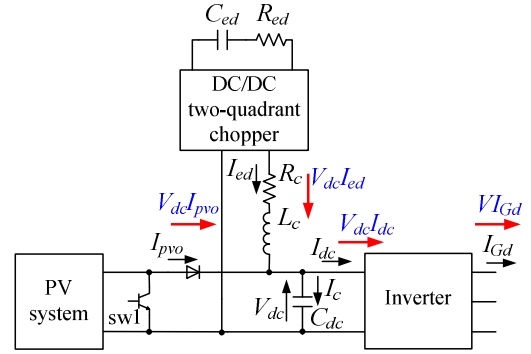


Fig.4 Power flow in the DC side

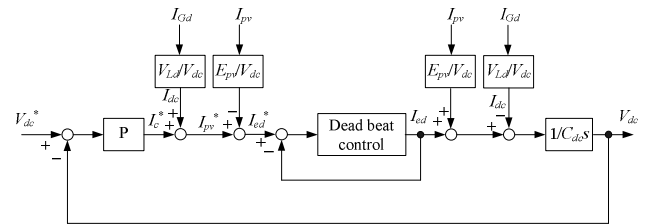


Fig.5 Block diagram of the control of PL unit side

Fig.5 shows a block diagram of the PL unit control. The digital deadbeat control is applied to control the output current of the PL unit.

### D. Digital Deadbeat Control of PL Unit

In Fig.5, the output current reference  $I_{ed}^*$  for leveling the fluctuation of PV output is calculated to keep voltage of DC bus constant. Then, the digital deadbeat control[6] is applied to the PL unit in order to obtain quick response of output current. In the PWM control of the two-quadrant chopper, the optimum duty ratio per cycle of the digital control is calculated by the state-space averaging method.  $sw2$  and  $sw3$  are alternatively switched according to the calculated duty ratio. Operation of  $sw2$  and  $sw3$  is shown in Fig.6.

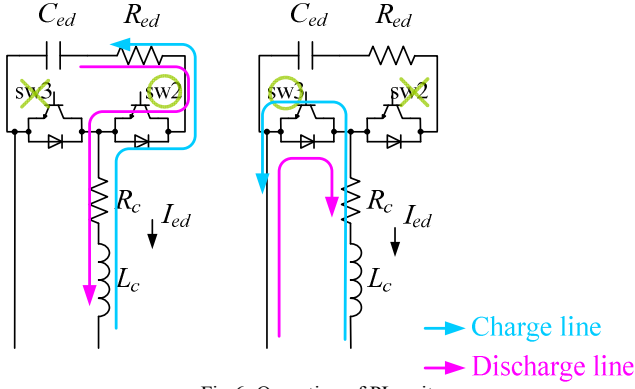


Fig.6. Operation of PL unit

State equations with respect to on and off operations are as follows.

$$T_{ON} : \frac{d}{dt} \begin{bmatrix} i_{ed} \\ v_{ed} \end{bmatrix} = \begin{bmatrix} -\frac{R_c + DR_{ed}}{L_c} & \frac{1}{L_c} \\ -\frac{1}{C_{ed}} & 0 \end{bmatrix} \begin{bmatrix} i_{ed} \\ v_{ed} \end{bmatrix} + \begin{bmatrix} -\frac{1}{L_c} \\ 0 \end{bmatrix} V_{dc} \quad (18)$$

$$T_{OFF} : \frac{d}{dt} \begin{bmatrix} i_{ed} \\ v_{ed} \end{bmatrix} = \begin{bmatrix} -\frac{R_c}{L_c} & 0 \\ 0 & 0 \end{bmatrix} \begin{bmatrix} i_{ed} \\ v_{ed} \end{bmatrix} + \begin{bmatrix} -\frac{1}{L_c} \\ 0 \end{bmatrix} V_{dc} \quad (19)$$

In accordance with the state-space averaging method, the weighted state equation by the duty ratio  $d$  is obtained from (18) and (19).

$$\begin{aligned} \frac{d}{dt} \begin{bmatrix} \bar{i}_{ed} \\ \bar{v}_{ed} \end{bmatrix} &= \begin{bmatrix} -\frac{dR_c + dR_{ed} + (1-d)R_c}{L_c} & \frac{d}{L_c} \\ -\frac{d}{C_{ed}} & 0 \end{bmatrix} \begin{bmatrix} \bar{i}_{ed} \\ \bar{v}_{ed} \end{bmatrix} + \begin{bmatrix} -\frac{d + (1-d)}{L_c} \\ 0 \end{bmatrix} \bar{V}_{dc} \\ &= \begin{bmatrix} -\frac{R_c + dR_{ed}}{L_c} & \frac{d}{L_c} \\ -\frac{d}{C_{ed}} & 0 \end{bmatrix} \begin{bmatrix} \bar{i}_{ed} \\ \bar{v}_{ed} \end{bmatrix} + \begin{bmatrix} -\frac{1}{L_c} \\ 0 \end{bmatrix} \bar{V}_{dc} \end{aligned} \quad (20)$$

Each value is divided into steady-state value and minute change value, defined by the following equations:

$$d \equiv D + d_p, \quad \bar{i}_{ed} \equiv I_{ed} + i_{edp}, \quad \bar{v}_{ed} \equiv V_{ed} + v_{edp}, \quad \bar{V}_{dc} \equiv V_{dc} + v_{dcp}$$

Substituting (20), (21) is obtained.

$$\begin{aligned} \frac{d}{dt} \begin{bmatrix} I_{ed} + i_{edp} \\ V_{ed} + v_{edp} \end{bmatrix} &= \begin{bmatrix} -\frac{R_c + (D + d_p)R_{ed}}{L_c} & \frac{D + d_p}{L_c} \\ -\frac{D + d_p}{C_{ed}} & 0 \end{bmatrix} \begin{bmatrix} I_{ed} + i_{edp} \\ V_{ed} + v_{edp} \end{bmatrix} \\ &+ \begin{bmatrix} -\frac{1}{L_c} \\ 0 \end{bmatrix} (V_{dc} + v_{dcp}) \end{aligned} \quad (21)$$

On other hand, (22) is given about steady state.

$$\frac{d}{dt} \begin{bmatrix} I_{ed} \\ V_{ed} \end{bmatrix} = \begin{bmatrix} -\frac{R_c + DR_{ed}}{L_c} & \frac{D}{L_c} \\ -\frac{D}{C_{ed}} & 0 \end{bmatrix} \begin{bmatrix} I_{ed} \\ V_{ed} \end{bmatrix} + \begin{bmatrix} -\frac{1}{L_c} \\ 0 \end{bmatrix} V_{dc} \quad (22)$$

To analyze minute change, (23) can be derived by calculating difference between (21) and (22).

$$\begin{aligned} \frac{d}{dt} \begin{bmatrix} i_{edp} \\ v_{edp} \end{bmatrix} &= \begin{bmatrix} -\frac{R_c + DR_{ed}}{L_c} & \frac{D}{L_c} \\ -\frac{D}{C_{ed}} & 0 \end{bmatrix} \begin{bmatrix} i_{edp} \\ v_{edp} \end{bmatrix} + \begin{bmatrix} -\frac{R_{ed}I_{ed} + V_{ed}}{L_c} \\ -\frac{I_{ed}}{C_{ed}} \end{bmatrix} d_p \\ &+ \begin{bmatrix} -\frac{1}{L_c} \\ 0 \end{bmatrix} v_{dcp} \end{aligned} \quad (23)$$

(23) is the linearized state equation. After replacing the Laplace operator  $s$  to the differential operator, the z-transform is performed using the backward difference method in (24).

$$s = \frac{1 - z^{-1}}{T} \quad (24)$$

$$\frac{1 - z^{-1}}{T} i_{edp} = -\frac{R_c + DR_{ed}}{L_c} i_{edp} + \frac{D}{L_c} v_{edp} - \frac{R_{ed}I_{ed} - V_{ed}}{L_c} d_p - \frac{1}{L_c} v_{dcp} \quad (25)$$

$$\frac{1 - z^{-1}}{T} v_{edp} = -\frac{D}{C_{ed}} i_{edp} - \frac{I_{ed}}{C_{ed}} d_p \quad (26)$$

To organize the above equation, (27) and (28) are obtained.

$$\begin{aligned} \left\{ 1 + \frac{(R_c + DR_{ed})T}{L_c} \right\} i_{edp} &= z^{-1} i_{edp} + \frac{DT}{L_c} v_{edp} \\ &- \frac{(R_{ed}I_{ed} - V_{ed})T}{L_c} d_p - \frac{T}{L_c} v_{dcp} \end{aligned} \quad (27)$$

$$v_{edp} = z^{-1} v_{edp} - \frac{DT}{C_{ed}} i_{edp} - \frac{TI_{ed}}{C_{ed}} d_p \quad (28)$$

These are substituted into the discrete time system equation.

$$\begin{aligned} \left\{ 1 + \frac{(R_c + DR_{ed})T}{L_c} \right\} i_{edp}(k) &= i_{edp}(k-1) + \frac{DT}{L_c} v_{edp}(k) \\ &- \frac{(R_{ed}I_{ed} - V_{ed})T}{L_c} d_p(k) - \frac{T}{L_c} v_{dcp}(k) \end{aligned} \quad (29)$$

$$v_{edp}(k) = v_{edp}(k-1) - \frac{DT}{C_{ed}} i_{edp}(k) - \frac{TI_{ed}}{C_{ed}} d_p(k) \quad (30)$$

Substituting (27) for (26), (31) is obtained.

$$\begin{aligned} i_{edp}(k) &= \frac{L_c C_{ed}}{L_c C_{ed} + (R_c + DR_{ed})TC_{ed} + (DT)^2} i_{edp}(k-1) \\ &+ \frac{TC_{ed}D}{L_c C_{ed} + (R_c + DR_{ed})TC_{ed} + (DT)^2} v_{edp}(k-1) \\ &- \frac{T^2 DI_{ed} + (R_{ed}I_{ed} - V_{ed})TC_{ed}}{L_c C_{ed} + (R_c + DR_{ed})TC_{ed} + (DT)^2} d_p(k) \\ &- \frac{TC_{ed}}{L_c C_{ed} + (R_c + DR_{ed})TC_{ed} + (DT)^2} v_{dcp}(k) \end{aligned} \quad (31)$$

Therefore, (31) becomes

$$d_p(k) = \frac{1}{k_3} \{ i_{edp}(k) - k_1 i_{edp}(k-1) - k_2 v_{edp}(k-1) - k_4 v_{dcp}(k) \} \quad (32)$$

,where  $k_1$ ,  $k_2$ ,  $k_3$  and  $k_4$  are coefficients of steady state values in (31).

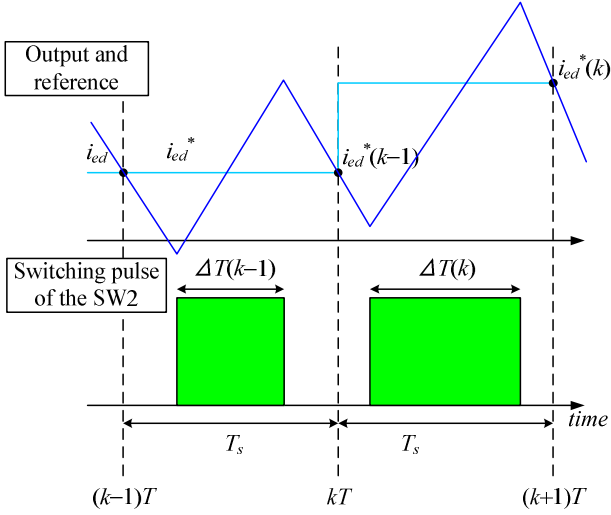


Fig.7 Principle of deadbeat control

Since the  $p$  components are minute change values from the steady-state value, (32) becomes the following equation.

$$D(k) - D(k-1) = \frac{1}{k_3} \begin{bmatrix} I_{ed}(k) - I_{ed}(k-1) \\ -k_1 \{ I_{ed}(k-1) - I_{ed}(k-2) \} \\ -k_2 \{ V_{ed}(k-1) - V_{ed}(k-2) \} \\ -k_4 \{ V_{dc}(k) - V_{dc}(k-1) \} \end{bmatrix} \quad (33)$$

From (33), it is possible to determine the optimal PWM duty ratio  $D(k)$  by detected  $I_{ed}, V_{ed}, V_{dc}$ . And the detected output current of PL unit  $I_{ed}$  can follow the reference value  $I_{ed}^*$  with one sample delay. The Principle of the deadbeat control is shown in Fig.6. By outputting the optimal pulse width  $D(k)$ , the output current can be matched with the current reference at each sampling time.

### III. SIMULATION

#### A. Simulation Pattern

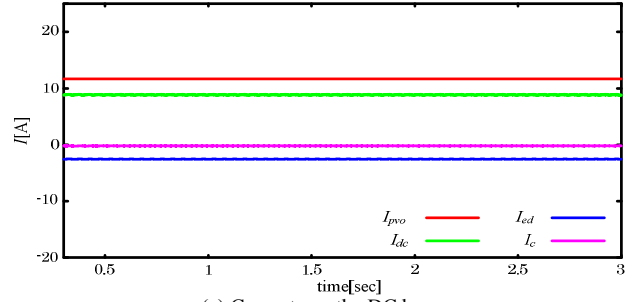
Simulation was performed using the circuit model of Fig.1. Parameters of the circuit are shown in Table 1. Computation time for all the control including P, PI and the deadbeat control is 100 $\mu$ s. Carrier frequency of the chopper and inverter is 10kHz.

The simulations are performed about typical steady state and transient cases. The steady state characteristic is divided into two patterns, which are continuous discharge pattern and continuous charge pattern from/to the super capacitor. The transient characteristic is executed in case of change to the charge pattern from the discharge pattern with PV output fluctuation, and in case that load suddenly changes by step.

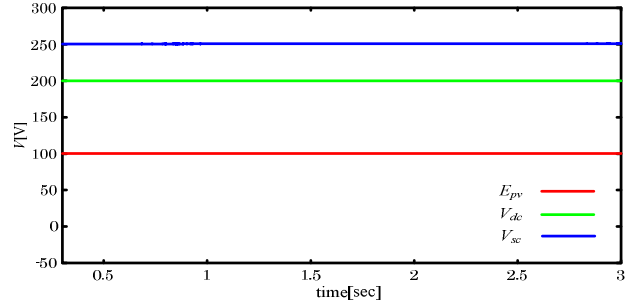
In the steady state case, the output voltage  $E_{pv}$  from the PV system is assumed to be constant. And in the transient case, to imitate the small output fluctuation of PV system, a random function is incorporated to the output voltage  $E_{pv}$ . Thus a condition about charge or discharge pattern often changes according to the output of the PV system.

TABLE I. PARAMETERS OF THE CIRCUIT.

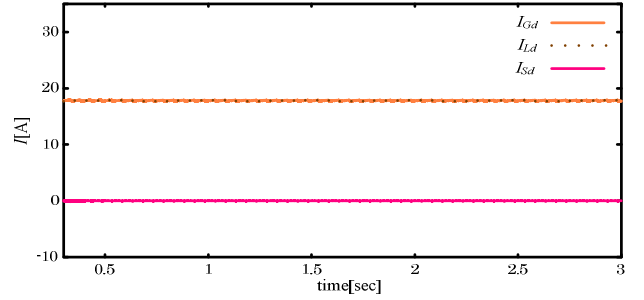
| Line voltage | 100 V           | Frequency  | 60 Hz           |
|--------------|-----------------|------------|-----------------|
| $R_S$        | 0.25 $\Omega$   | $L_S$      | 218 $\mu$ H     |
| $R_G$        | 0.15 $\Omega$   | $L_G$      | 131 $\mu$ H     |
| $R_L$        | 5.00 $\Omega$   | $L_L$      | 4.36 mH         |
| $R_c$        | 10.0 m $\Omega$ | $L_c$      | 10.0 mH         |
| $C_{ed}$     | 10.0 F          | $R_{ed}$   | 0.2 $\Omega$    |
| $C_{pv}$     | 5000 $\mu$ F    | $R_{pv}$   | 10.0 m $\Omega$ |
| $L_{pv}$     | 10.0 mH         | $V_{dc}^*$ | 200 V           |



(a) Currents on the DC bus



(b) Voltages on the DC bus



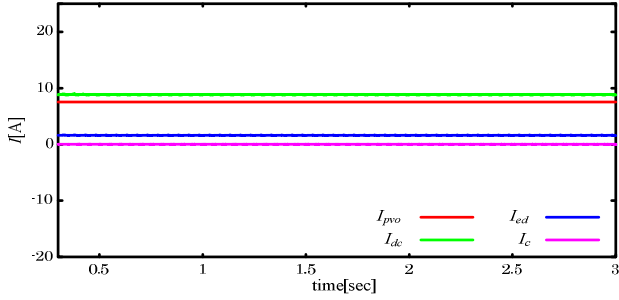
(c) Active current on the AC bus

Fig.8 Steady state in case of the charge to a super capacitor

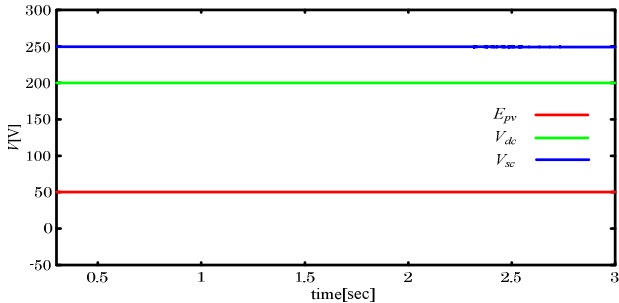
#### B. Steady State Characteristics

Figs.8-10 are simulation results on the steady state. Fig.8 shows a result of continuous charge with a constant output of the PV system.

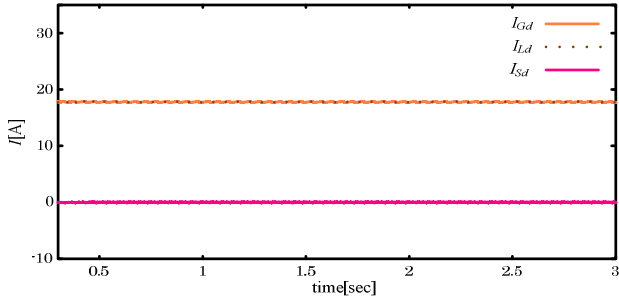
Fig.8(a) shows currents on the DC bus. Input current  $I_{dc}$  of the inverter is controlled to balance output active power for the load on AC line. Output current  $I_{pvo}$  of the PV system keeps constant and is larger than  $I_{dc}$  ( $I_{pvo} > I_{dc}$ ). In this case, the surplus power flows to a super capacitor to charge ( $I_{ed} < 0$ ). And  $I_c$  becomes 0 when  $V_{dc}$  is constant. Fig.8(b) shows voltages on the DC bus. Output voltage  $E_{pv}$  of the PV system is constant at 100V and DC bus voltage  $V_{dc}$  can be controlled to keep constant at 200V by



(a) Currents on the DC bus



(b) Voltages on the DC bus



(c) Active current on the AC bus

Fig.9 Steady state in case of the discharge from a super capacitor

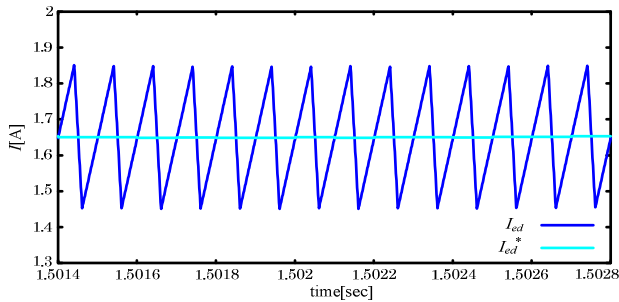
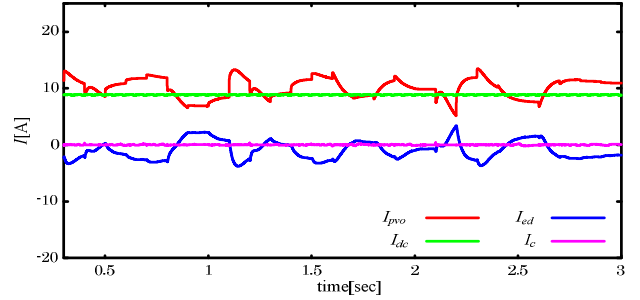


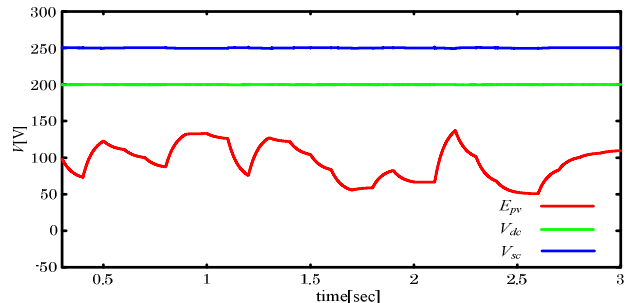
Fig.10 Enlarged figure of output current  $I_{ed}$  in Fig.9(a)

the DC bus voltage control. Voltage  $V_{sc}$  of the super capacitor increases a little due to the power charge to the capacitor. Fig.8(c) shows active components of currents on the AC bus. Active power supplied from the main power line becomes 0, because it is controlled to minimize the power consumption of the main power line. In this case, all the active power to the load is supplied from the DG. Thus, the effective power balance between the DG, the load and the main power line on AC bus is achieved.

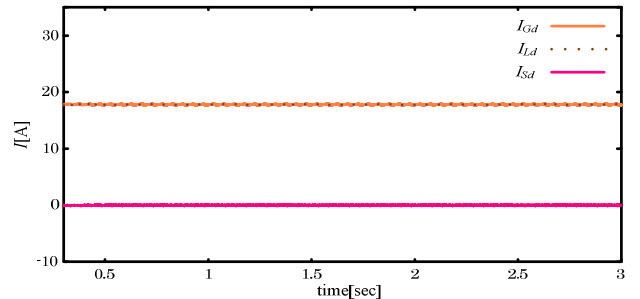
Fig.9 shows a result of continuous discharge with a constant output of the PV system. Fig.9(a) shows currents



(a) Currents on the DC bus



(b) Voltages on the DC bus



(c) Active current on the AC bus

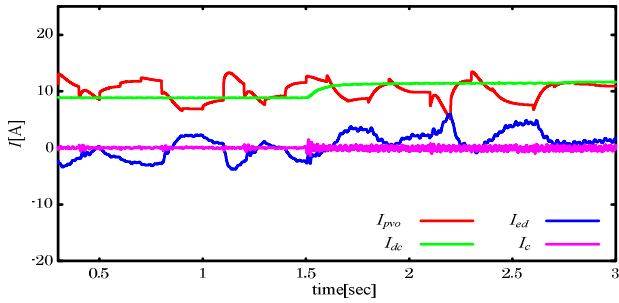
Fig.11 Transient response with the fluctuation of PV output

on the DC bus. Input current  $I_{dc}$  of the inverter is controlled to balance output active power for the load on AC line. Output current  $I_{pvo}$  of the PV system is smaller than  $I_{dc}$  ( $I_{pvo} < I_{dc}$ ). In this case, the shortage power for the load is supplied from a super capacitor. Thus the super capacitor discharges ( $I_{ed} < 0$ ). Fig.9(b) shows voltages on the DC bus. Output voltage  $E_{pv}$  of the PV system is constant at 50V and DC bus voltage  $V_{dc}$  can be controlled to keep constant at 200V by the DC bus voltage control. Voltage  $V_{sc}$  of the super capacitor decreases a little due to the power discharge from the capacitor. Fig.9(c) shows active components of currents on the AC bus. In this case, all the active power to the load is supplied from the DG. Thus, the effective power balance between the DG, the load and the main power line on AC bus is achieved the same as the case of Fig.8.

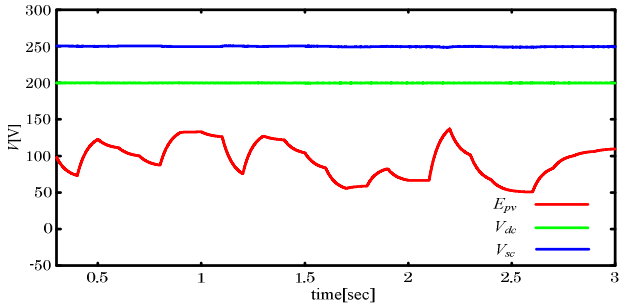
Fig.10 shows a enlarged waveform of output current  $I_{ed}$  in Fig.9(a) for certain short period. Output current  $I_{ed}$  of the PL unit can follow to the reference  $I_{ed}^*$  at each sampling time according to the deadbeat control theory in Fig.7.

### C. Transient Characteristic

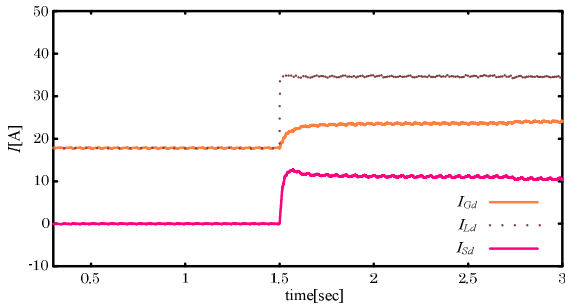
Figs.11-13 are simulation results on the transient with the PV fluctuation.



(a) Currents on the DC bus



(b) Voltages on the DC bus



(c) Active current on the AC bus

Fig.12 Transient response with the load change (50%→100%)

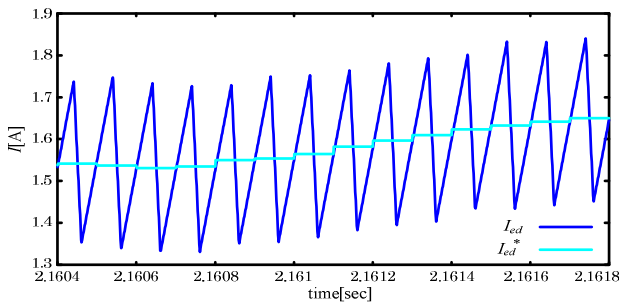


Fig.13 Enlarged figure of output current  $I_{ed}$  in Fig.12(a)

Fig.11 shows a result of transient response in case with irregular output of the PV system by weather condition change. In Fig.11(a), Input current  $I_{dc}$  of the inverter is controlled to balance output active power for the load on AC line and  $I_c$  becomes 0 when  $V_{dc}$  is constant. Output current  $I_{pvo}$  of the PV system has fluctuation by the condition change. Therefore output  $I_{ed}$  of the PL unit repeatedly changes between the charge pattern ( $I_{ed} < 0$ ) and the discharge ( $I_{ed} > 0$ ) pattern to keep  $I_{dc}$  constant. In Fig. 11(b), DC bus voltage  $V_{dc}$  can be controlled to keep constant at 200V by the DC bus voltage control. Output voltage  $E_{pv}$  of the PV system irregularly changes by the condition change and  $V_{sc}$  of the super capacitor repeats the

increase or decrease according to the fluctuation of  $E_{pv}$ . Fig.11(c) shows active components of currents on the AC bus. All the active power to the load is appropriately supplied from the DG without depending on the PV fluctuation. Thus, the result is the same as the cases of steady state in Figs.8-9.

Fig.12 shows a result of transient response in case with the load change by step and the irregular output of the PV system. The load changes two-fold at  $t = 1.5$ s. The fluctuation condition is the same as the case in Fig.11. In Fig.12(a),  $I_{dc}$  increases and keeps constant, which is the rated maximum, after  $t = 1.5$ s because the load increases.  $I_{ed}$  of the PL unit properly repeats the increase or decrease in order to keep balance the power flow. As a result, DC bus voltage  $V_{dc}$  becomes constant at 200V in spite of the load change and the PV fluctuation in Fig.12(b). In Fig.12(c), the active current  $I_{Ld}$  increases to double, however, output current  $I_{Gd}$  of the DG does not become double because it attains to the rated current. Therefore  $I_{Sd}$  flows to the load to compensate the deficit in the active power.

Fig.13 is a enlarged waveform of output current  $I_{ed}$  in Fig.12(a) for certain short period. Output current  $I_{ed}$  of the PL unit can follow to the reference  $I_{ed}^*$  at each sampling time by the deadbeat control.

#### IV. CONCLUSIONS

In this research, a new method of digital control in PL unit with a super capacitor is proposed. This method is a way for obtaining the optimal duty ratio of PWM from the linearized state equation. The power leveling with quick response by the digital dead-beat control was performed in the simulation. The control method was theoretically analyzed and excellent results in the typical situations were achieved by the simulations.

#### REFERENCES

- [1] H. Kakigano, M. Nomura, T. Ise, "Loss Evaluation of DC Distribution for Residential Houses Compared with AC System", *The 2010 International Power Electronics Conference (IPEC)*, pp.480-486, 2010
- [2] Y. Ito, Z. Yang, H. Akagi, "A Control Method of a Small-Scale DC Power System Including Distributed Generators"(in Japanese), *IEEJ Trans. on IA*, Vol. 126, No. 9, pp.1236-1241, 2006
- [3] K. Yukita, Y. Shimizu, Y. Goto, et al., "Study of AC/DC Power Supply System with DGs using Parallel Processing Method", *The 2010 International Power Electronics Conference (IPEC)*, pp.722-725, 2010
- [4] S. Hamasaki, M. Tsuji, et al., "A Study on Power Flow Control for Distributed Generator with EDLC", *International Symposium on Power Electronics, Electrical Drives Automation and Motion (SPEEDAM)*, pp.902-907, 2010
- [5] A. Prasai, A. Paquette, et al., "Minimizing Emissions in Microgrids While Meeting Reliability and Power Quality Objectives", *The 2010 International Power Electronics Conference (IPEC)*, pp.726-733, 2010
- [6] S. Hamasaki and A. Kawamura, "Improvement of Current Regulation of Line-Current-Detection-Type Active Filter Based on Deadbeat Control", *IEEE Trans. on IA*, vol. 39, No.7, pp.536-541, 2003